Controlling Nanoscale Friction through the Competition between Capillary Adsorption and Thermally Activated Sliding

Christian Greiner,[†,§] Jonathan R. Felts,[‡] Zhenting Dai,[‡] William P. King,[‡] and Robert W. Carpick[†,*]

[†]Department for Mechanical Engineering and Applied Mechanics, University of Pennsylvania, 112 Towne Building, 220 South 33rd Street, Philadelphia, Pennsylvania 19104, United States, and [‡]Department of Mechanical Science and Engineering, University of Illinois at Urbana—Champaign, 242 Mechanical Engineering Building, 1206 West Green Street, Urbana, Illinois 61801, United States. [§]Present address: Karlsruhe Institute of Technology, Institute for Applied Materials (IAM), Kaiserstrasse 12, 76131 Karlsruhe, Germany.

ABSTRACT

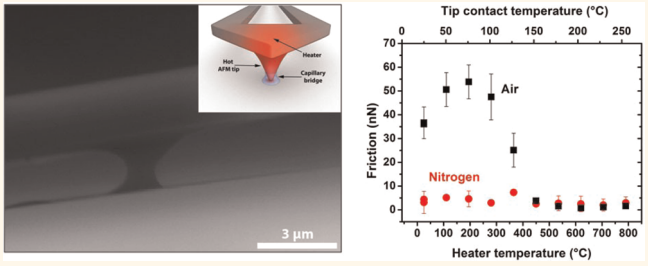

We demonstrate measurement and control of nanoscale single-asperity friction by using cantilever probes featuring an *in situ* solid-state heater in contact with silicon oxide substrates. The heater temperature was varied between 25 and 790 °C. By using a low thermal conductivity sample, silicon oxide, we are able to vary tip temperatures over a broad range from 25 ± 2 to 255 ± 25 °C. In ambient atmosphere with ~30% relative humidity, the control of friction forces was achieved through the formation of a capillary bridge whose characteristics exhibit a strong dependence on temperature and sliding speed. The capillary condensation is observed to be a thermally activated process, such that heating in ambient air caused friction to increase due to the capillary bridge nucleating and growing. Above tip temperatures of ~100 ± 10 °C, friction decreased drastically, which we attribute to controllably evaporating water from the contact at the nanoscale. In contrast, in a dry nitrogen atmosphere, friction was not affected appreciably by temperature changes. In the presence of a capillary, friction decreases at higher sliding speeds due to disruption of the capillary; otherwise, friction increases in accordance with the predictions of a thermally assisted sliding model. In ambient atmospheres, the rate of increase of friction with sliding speed at room temperature is sufficiently strong that the friction force changes from being smaller than the response at 76 ± 8 °C to being larger. Thus, an appropriate change in temperature can cause friction to increase at one sliding speed, while it decreases at another speed.

KEYWORDS: friction · AFM · silicon oxide · heated probes · sliding speed

Friction forces between materials can depend strongly on temperature, but the fundamental physical phenomena governing this are not well understood. Exploring such phenomena can potentially help shed light on the origins of friction and provide a means to control or modulate friction for desired applications, including micro- and nanoelectromechanical systems (MEMS/NEMS).[1−6] Tribological processes and the associated dissipation of energy are complex and ubiquitous in nature. Among the many challenges include the fact that when macroscopic objects slide in contact, the interface is not continuous but composed of many asperities. It is therefore desirable to conduct fundamental studies of friction, including of the temperature dependence, at the nanoscale.[7,8] The extremely sharp tip of an atomic force microscope (AFM) enables the study of an individual nanoscale asperity,[9,10] enabling definitive identification and analysis of the underlying physical processes (Figure 1).

Several AFM-based experiments have been conducted to explore the temperature dependence of nanoscale friction for a variety of materials at temperatures up to ~480 °C. These experiments typically involved heating either the sample itself or heating the entire apparatus in which the experiment is situated.[1,2,4,5,11−14] A recent publication has demonstrated the feasibility and advantage of investigating single-asperity friction by means of a heated AFM cantilever probe.[15] This *in situ* technique allows experimental time scales for temperature variation that are ~10^6 times faster than previous approaches (with temperature changes in the submillisecond regime[16]). An observed increase in friction with increased temperature, only seen in humid environment, suggested that thermally activated formation of a capillary was occurring and strongly affecting friction. Using this hypothesis, the kinetics of thermally induced capillary condensation could then be studied in real-time.[15] Estimated tip

* Address correspondence to carpick@seas.upenn.edu.

Received for review February 27, 2012 and accepted April 20, 2012.

Published online April 20, 2012
10.1021/nn300869w

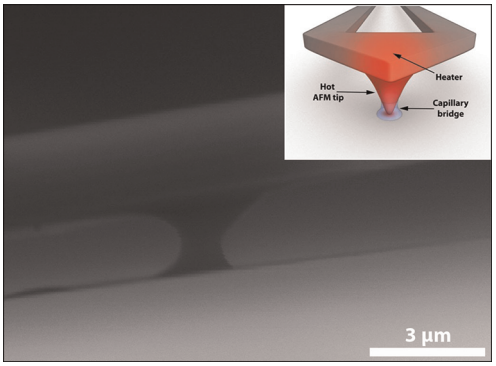

Figure 1. Environmental scanning electron microscopy image of a capillary bridge between the tip of a thermal AFM probe and a hydrophilic substrate. The ESEM image highlights the capillary nucleated between the tip and substrate. Inset: Schematic of the thermal probe. The heating around the tip−substrate contact is highly localized. Cantilever heating is achieved through Joule heating of the lower-doped heater region at the end of the cantilever.

temperatures up to just ~120 ± 20 °C were used. A key advantage of this technique is that one can rapidly and repeatedly separate the temperature effects from others like tip wear and measure more rapid kinetic processes. However, it is desirable to further expand the temperature range to probe for additional phenomena, including seeking evidence for capillary evaporation, which would provide definitive evidence that indeed capillary formation was responsible for the observed friction phenomena.

While ultrahigh vacuum (UHV) conditions are ideal for friction studies by allowing nearly contamination-free surfaces, contacts in almost all applications do not function in UHV but in ambient conditions. Thus, we focus here on measurements in humid ambient and dry nitrogen atmospheres to determine the effect of humidity on friction and to further explore the properties of nanoscale capillary formation. Previous results were obtained on silicon substrates with a thin native oxide.[15] The thermal conductivity of silicon was the key factor limiting the tip−sample contact temperature to approximately 120 ± 20 °C.[15,17] In this work, we instead used silicon oxide as a substrate material. Its lower thermal conductivity compared to silicon prevents the tip's heat from being transported as rapidly into the bulk of the sample, enabling the contact region to reach a substantially higher steady-state temperature. We study the dependence of friction with temperature over this range and explore the modulation of friction forces with temperature as well as with sliding speed.

Together with silicon, silicon oxide is an extremely important material for nano- and microelectromechanical system (NEMS and MEMS) applications, where control over adhesion, friction, and wear is a major concern.[18] The behavior of NEMS/MEMS at different temperatures is particularly important as these systems need to operate in harsh environments for aerospace applications, in propulsion systems, and in

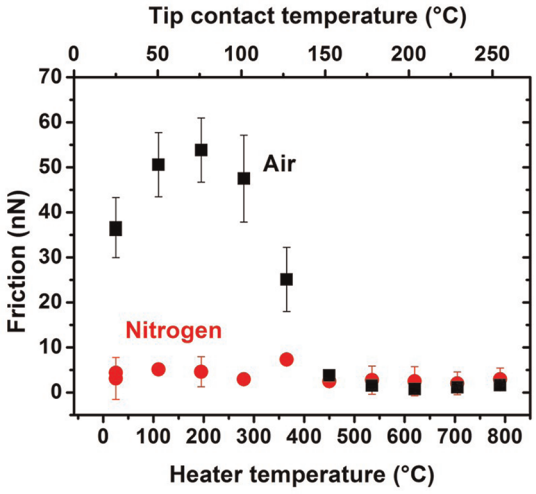

Figure 2. Friction as a function of temperature at constant normal load between a Si tip and a silicon oxide substrate. Experiments were performed at a constant normal load of 112 nN and a sliding speed of 400 nm/s. Heater temperatures were chosen in a randomly alternating order. Results from measurements in humid ambient air (black squares) and dry nitrogen atmosphere (red circles).

switches where a high current density can heat device components appreciably.[19,20] While silicon-based MEMS, in general, are not well-suited for harsh environments and other material choices are being pursued,[21] the investigation of the adhesion and friction behavior of silicon and silicon oxide at elevated temperatures is of great importance.

RESULTS AND DISCUSSION

Friction forces were measured in both humid ambient air and in dry nitrogen atmosphere. An example is shown in Figure 2. Similar to our results on silicon substrates (with native oxide),[15] initially, friction increased upon heating above room temperature in humid air. However, when heater temperatures exceeded 250 °C (tip contact temperature ≈ 90 ± 10 °C), friction forces started to decrease drastically and from a heater temperature of 450 °C (tip contact temperature ≈ 150 ± 15 °C) onward remained at very small values. They were approximately one-seventh of the friction values found at room temperature (35 nN *vs* 5 nN). The behavior in dry nitrogen was different: Friction forces were nearly independent of temperature and had the same magnitude as the ones in humid air at higher heater temperatures (~4−6 nN).

The same trend of first increasing and then drastically decreasing friction forces with temperature in humid air was also found when measuring as a function of load. These results are presented in Figure 3 for six representative temperatures; the complete data set is presented in the Supporting Information. Performing the same experiments in dry nitrogen again revealed that friction was independent of temperature and at much smaller absolute values than in a humid

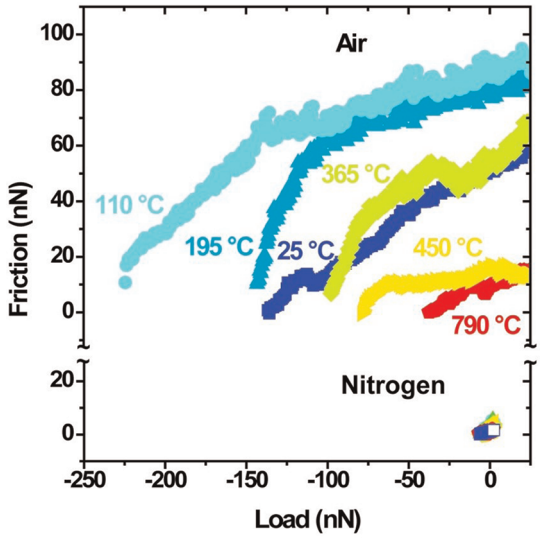

Figure 3. Friction as a function of normal load between a Si tip and a silicon oxide substrate. Friction was measured while the normal force was decreased until the tip pulled off from the substrate. The heater temperatures were chosen in an alternating order. The sliding speed was 400 nm/s. Results from measurements in ambient and dry nitrogen atmosphere for six representative temperatures. The complete data set is presented in the Supporting Information.

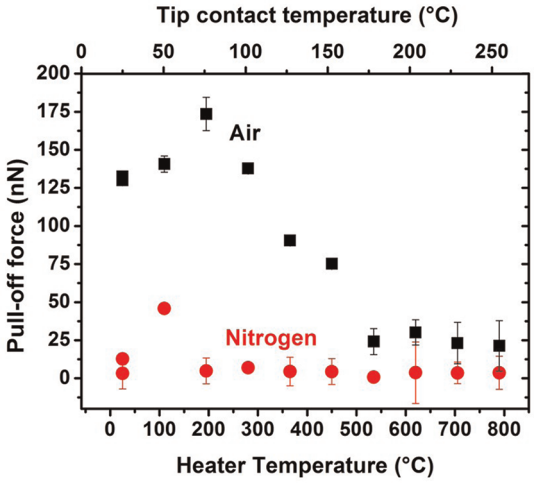

Figure 4. Temperature dependence of the pull-off force for a Si tip in contact with a silicon oxide substrate. As with the other experiments, the heater temperatures were chosen in an alternating order. Results from measurements in humid ambient air (black squares) and dry nitrogen atmosphere (red circles).

environment. The adhesion values (the point where the tip pulls off from the substrate) determined from Figure 3 show similar behavior. In humid air, adhesion first increased and started to decrease once higher heater temperatures (above ~250 °C) were reached. In dry nitrogen, there was no variation with temperature. Individual force–separation measurements of the adhesion force in both atmospheres yielded the same behavior (Figure 4). The pull-off forces in air were slightly higher than those in nitrogen.

In our previous experiments with silicon substrates, measurements at different sliding speeds enabled us to analyze the kinetics of capillary condensation.[15] Figure 5 shows experiments with sliding speeds between 40 and 7800 nm/s for the SiO_2 substrate. In humid air (Figure 5a) and for the first two heater temperatures (25 and 195 °C), friction forces initially decreased slightly, and after a certain temperature-dependent critical sliding speed (v_c) was reached, friction forces started to increase, in the room temperature case drastically (more than a factor of 3). For the two higher heater temperatures (450 and 705 °C), friction forces were lower overall, consistent with Figure 3. Friction increased with sliding speed, starting from the lowest one, but increased only marginally over the range of sliding speeds tested. In dry nitrogen (Figure 5b), friction forces increased slightly with sliding speed, and for all four heater temperatures, the same trend and force magnitudes (about the same as for the two higher temperatures in humid air) were found.

All data presented above can be consistently explained as follows:[15] Due to the hydrophilic nature of

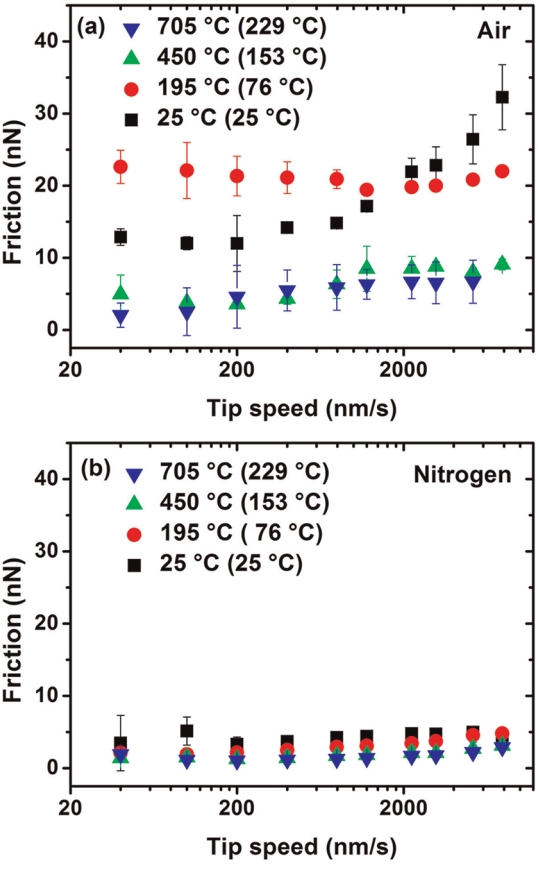

Figure 5. Friction as a function of sliding speed and temperature between a Si tip and a silicon oxide substrate. The sliding speed was varied between 40 and 7800 nm/s. Measurements were performed for four different heater temperatures: room temperature, 195, 450, and 705 °C (estimated tip temperatures: 25, 76, 153, and 229 °C). (a) Results from humid ambient and (b) dry nitrogen atmosphere.

tip and substrate, a capillary bridge is nucleated between the two if the atmosphere is moist enough, as is the case for humid ambient air (RH ≈ 25−35%). Other experiments[22−24] as well as Monte Carlo modeling[25−27] demonstrate the existence of capillary condensation at nanoscale tip−sample contacts. Liquid bridges between silicon AFM probes and silicon or gold-coated silicon substrates were directly imaged in environmental scanning electron microscopy (ESEM) previously by other groups[28,29] and recently by us, with the same type of thermal cantilevers as used for the present studies (Figure 1). Moreover, capillary formation is a thermally activated process.[13,15] The exact nature of the activated process may involve two aspects. First, capillary condensation, as a first-order phase transition, could have its own free energy barrier. In highly confined situations, the barrier can depend strongly on the geometry.[30] In addition, as the water vapor close to the tip is exposed to the confined region, the innermost vapor molecules are repelled by the corner walls between tip and substrate, locally squeezing the water molecules together and increasing their density. This might cause a slight increase in density and leaving them at a state between the binodal and spinodal in the phase diagram so that a phase transition requires overcoming an energy barrier.

Second, thermally activated desorption and diffusion of contaminant species typically present on surfaces exposed to ambient conditions will render surface sites available for nucleation of the meniscus. Higher temperatures help to overcome these activation barriers more rapidly, leading to more fully developed capillaries. Another aspect to be considered is the transport of water to the nanoscopic contact. This was recently described by Knudsen diffusion or by the surface adsorption and transport of water molecules.[24] Both mechanisms are thermally activated so that it is expected that temperature changes will influence adhesion and friction forces.

All of these mechanisms result initially in capillaries that grow as the temperature is increased from room temperature. The presence of the capillary bridge adds to the normal force between tip and substrate due to the associated Laplace pressure and surface tension.[31,32] This is why the absolute friction forces were larger in humid air than in dry nitrogen atmosphere (Figures 2 and 3), where there was no (or very little) moisture present so that no capillary could condense. As larger capillaries form with higher temperature, friction and adhesion forces increase in humid air with temperature. In a previous publication,[15] where measurements on silicon substrates were performed, this was the only trend observed. With the SiO_2 substrates investigated here, substantially higher tip−substrate contact temperatures were reached due to the lower thermal conductivity of SiO_2 compared to bare silicon (λ(Si) = 1.3−1.48 W/cm·K; $\lambda(SiO_2)$ = 0.014 W/cm·K). Once the tip contact temperature exceeded values of ∼100 ± 10 °C, we hypothesize that the capillary simply started to become smaller as water was evaporated from the contact.

It is difficult to precisely describe the process by which water is leaving the contact. The desorption of water from silica surfaces has been studied previously. It was observed that the desorption starts at around 100 °C, and desorption of the last monolayer is completed at roughly 400 °C.[33] As well, a study of the activation energy for desorption of water from porous silica gels with different pore sizes (between 2 and 10 nm) found that the activation energy increases with decreasing pore size.[34] These results highlight that the desorption behavior of water may change in nanoscale confinements, an effect further complicating a precise description of the processes leading to the friction reduction for tip contact temperatures between 100 ± 10 and 150 ± 15 °C. In addition, the temperature gradient in the tip and the temperature distribution between the heater and the substrate (as well as in the substrate around the tip) are complex and non-uniform.[17] This is especially true in the presence of a capillary bridge, which will alter the temperature distribution. Such a system has not been modeled before, and this remains a task for future research. The thermal tip methods we describe here provide a promising avenue for conducting such studies.

Previous experiments with an environmental scanning electron microscope by Weeks *et al.*[28,29] have demonstrated that the capillary between tip and substrate can be much larger than predicted by classical theory based on the Kelvin radius (several hundreds of nanometers *vs* only a few nanometers). To obtain further insight into the nature of the capillary in our case, we studied the capillary bridge between the thermal AFM probe and substrate in an ESEM (FEI Quanta 600 FEG Mark II). For these investigations, the substrate was cooled and the partial pressure of water inside the electron microscope was increased through a differential pumping process. For the ESEM image shown in Figure 1, the substrate temperature was 2 °C and the partial pressure of water was 5.1 Torr. A voltage of 1 V was applied to the cantilever. While a detailed description of our ESEM experiments will be published separately, an astonishingly large capillary (several hundreds of nanometers) as described by Weeks *et al.*[28,29] was also found for our contact. Therefore, it is possible that the size of the capillary in the AFM experiments is significantly larger than predicted.

As the heater reached temperatures of 250 °C and above (tip temperature of ∼90 ± 10 °C and above), friction and adhesion forces started to decrease abruptly (Figures 2 and 4). It is hypothesized that this is a result of evaporation of the water. Once all of the water was driven out of the contact, there was no

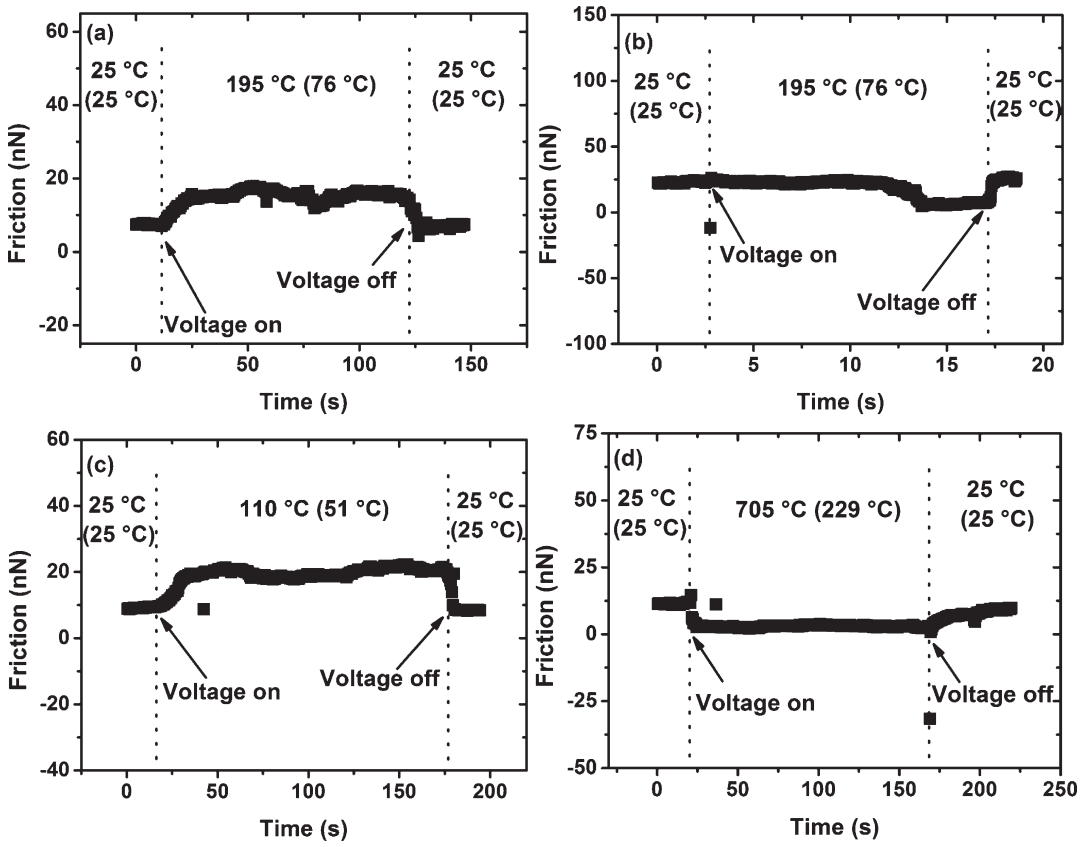

Figure 6. Real-time heating experiments in ambient for a Si tip sliding on a silicon oxide substrate. The temperature of the heater was changed while scanning. The experiment started with the cantilever being at room temperature. Then the voltage corresponding to (a,b) 195 °C, (c) 110 °C, and (d) 705 °C heater temperature (tip temperatures are given in parentheses) was switched on. After a steady friction value is reached, the voltage was switched off again. Sliding speed was (a,c,d) 400 nm/s and (b) 5208 nm/s.

capillary component to add to friction and adhesion forces. Correspondingly, the absolute values for both were significantly lower than those at room temperature (where there was a capillary present).

The Prandtl–Tomlinson model[35–38] provides the classical picture of atomic-scale friction. Here, the tip sticks at metastable positions determined by local energy minima in the combined potential of the periodic lateral tip–sample interaction and the elastic components of the system (namely, the spring that supports the tip, the tip itself, and the deformed contact zone). Thermal activation assists in overcoming the barrier to the next metastable position, thus, friction is expected to decrease with temperature.[39] In this picture, at higher sliding speeds, less time is available at each metastable position to allow thermal activation to assist in sliding, and so starting from the low sliding speed limit, friction increases with speed.[37,40] Throughout this paper, sliding speed refers not to the instantaneous slipping speed of the tip but to the speed of the holder on the other end of the spring connected to the tip (*i.e.*, the base of the cantilever) with respect to the sample. When measuring on silicon substrates, we observed increasing friction with sliding speed for measurements in dry nitrogen atmosphere.[15] For our experiments on SiO_2 presented here, friction increased slightly with sliding speed in dry nitrogen (Figure 5b). The same is true for the regime of higher heater temperatures (450 and 705 °C) in humid air where all humidity was driven away from the contact and a true solid–solid contact behavior is expected. The data for the two other temperatures in humid air (25 and 195 °C) contradict the Tomlinson model. It can be explained as first brought forward by Riedo *et al.*[13,41,42] and seen in our previous experiments on silicon samples (with only a native oxide):[15] At higher sliding speeds, it becomes increasingly difficult for the capillary to follow the sliding contact, as limited by a critical sliding speed v_c. This can be a result of the capillary encountering defects that pin it to the substrate or regions of lower topography that break the capillary since it has to stretch to be maintained. Once the capillary is destroyed, there is a barrier for the nucleation of a new one. This corresponds to the points where the two lines for 25 and 195 °C in Figure 5a change their slope. It has been shown in the literature that the nucleation process follows Arrhenius kinetics.[13,15] This temperature dependence shifts the critical speed to larger values for higher temperatures, as observed in Figure 5a, where v_c is at approximately 250 nm/s at room temperature and 1550 nm/s at 195 °C heater temperature. At sliding

speeds exceeding the critical one, friction forces increase with speed, as is expected from the classical Tomlinson picture. In a publication by Sirghi,[24] it was shown that the adhesive force between a hydrophilic substrate and an AFM tip decreases as the lateral speed of the tip increases. These results are fully consistent with ours and were also explained by the time necessary to form the meniscus.[24]

The crossover between the data for 25 and 195 °C at a speed of approximately 1800 nm/s, inspired the following consideration: For silicon substrates, we were able to show[15] that it is possible to switch on and off capillary condensation in real-time by changing the temperature of the heater while scanning. This is a capability unique to this setup and only possible with this method of heating the contact directly at the nanoscale. With this capability in mind, one could take advantage of the above-mentioned crossover in the following way: By switching between room temperature and 195 °C in real-time in humid air, it should be possible to both increase and decrease friction forces, depending on sliding speed. The results of such an experiment are shown in Figure 6a,b. In Figure 6a, for a sliding speed of 400 nm/s (thus, much smaller than the 1800 nm/s crossover speed), friction forces increased upon heating as expected (by about a factor of 2.0). In Figure 6b, the speed was increased to 5208 nm/s, well above the crossover speed. After switching to the higher temperature, about 10 s passed before friction forces started to decrease and then reached a plateau, significantly below the initial values at room temperature (about a factor of 3.7). When the heating was stopped, friction forces almost immediately reached their previous higher values. These results, and the ones presented in Figure 6c,d for sliding speeds of 400 nm/s each and for heating to 110 and 705 °C, are fully consistent with the capillary condensation model discussed so far. At smaller sliding speeds and for heater temperatures below 250 °C, the capillary grows upon heating, thus friction increases (Figure 6c, d). In Figure 6d, we chose a heater temperature where, according to Figures 2 and 3, water was expected to leave the contact entirely. Thus, as expected, friction forces decreased with the higher temperature as brought forward by the Tomlinson model. The control experiments for these results performed in dry nitrogen can be found in the Supporting Information. They show the expected behavior of decreasing friction forces upon heating for all chosen temperatures and no effect of sliding speed.

The ability of switching friction forces and to nucleate and eliminate a meniscus *in situ* and in real-time depending on temperature and sliding speed as demonstrated here creates several new opportunities. Tip-based nanomanufacturing and nanolithography schemes that rely on chemical reactions could be controlled by turning the meniscus on and off, as well as by temperature itself.[43] NEMS/MEMS actuation could be controlled by the substantial, reversible change in friction forces that can be achieved.

CONCLUSIONS

We introduced a new way of controlling nanoscale friction by using AFM probes with a solid-state heater. In ambient atmosphere, a thermally activated capillary bridge formed between the tip and substrate, increasing friction and adhesion as temperature is increased up to a heater temperature of 250 °C (estimated tip temperature of 92 ± 10 °C). Beyond this temperature, water is driven away from the contact, reducing adhesion and friction forces substantially. No capillary component is left once the heater temperature reaches 450 °C (estimated tip temperature of 152 ± 15 °C), and consequently, friction and adhesion each remain constant as a function of increasing temperature, each at respective values significantly lower than those at room temperature.

A distinct dependence of friction on speed is found for different regimes of capillary formation because the capillary's ability to follow the sliding tip is kinetically limited. When the capillary is present, friction decreases slightly with speed until a temperature-dependent critical speed at which the capillary's size is maximally reduced by the sliding action. If capillary nucleation is suppressed by either high sliding speeds, high temperatures, or dry environments, then friction follows the Prandtl–Tomlinson model for solid–solid contact where friction increases with sliding speed.

Thus, the behavior at various fixed temperatures and during real-time temperature variation depends on temperature, speed, and environment. In humid conditions, with the appropriate choice of tip speed, it is possible to obtain a decrease or increase in friction in real-time by increasing the temperature. This behavior is suppressed in dry nitrogen where friction always decreases upon heating, independent of sliding speed, again consistent with the Prandtl–Tomlinson model.

The results demonstrate the fascinating potential of thermal AFM tips to probe phenomena at the nanoscale and also show the ability to control nanoscale friction, adhesion, and capillarity *in situ* and in real-time.

METHODS

The experiments were performed with silicon AFM probes featuring an *in situ* solid-state heater[44,45] relying on Joule heating of differently doped parts of the cantilever.[16] An electric current is driven through the cantilever circuit, which includes the two highly doped legs and the lightly doped heater region,

below which the tip is located. The higher electrical resistance allows the end of the cantilever to reach temperatures ranging from room temperature (RT) up to approximately 800 °C. The temperature was varied by applying a constant DC voltage across the cantilever legs *via* a function generator (model 33120A, Agilent Technologies, Santa Clara, CA) in combination with a scaling amplifier (HSA4101, NF Corporation, Yokohama, Japan). Calibration between heater temperature and supplied voltage was performed by micro-Raman experiments for each cantilever.[16,46] The error in these measurements was approximately ±10 °C.

Silicon (100) wafers with a 1 μm thick, thermally grown silicon dioxide layer served as sample material. The wafers were provided by Universitywafer (South Boston, MA). Prior to experiments, pieces were cut from the wafer and cleaned with piranha solution (5 parts H_2SO_4, 1 part H_2O_2) to remove all organic contamination. After removal from piranha, the substrates were rinsed with deionized water and blown dry with dry nitrogen gas. Contact angle measurements (Ramé-Hart instrument contact angle goniometer, Netcong, NJ) confirmed the hydrophilic nature of the surfaces after piranha cleaning (25° static contact angle with water) compared to the as-received SiO_2 wafers (62°).

The normal force constant of each cantilever was determined *in situ* at all heater temperatures by applying the reference cantilever method as described by Tortenese *et al.*[47,48] The reference cantilevers were obtained from Veeco (Santa Barbara, CA). The lateral spring constant of each cantilever was determined with a diamagnetic lateral force calibrator as described by Li *et al.*,[49] also at each heater temperature. The calibration in the lateral and normal direction had to be performed at each heater temperature as normal and lateral spring constants are a function of temperature due to changes in the elastic modulus of silicon with temperature and due to twisting and bending of the cantilevers upon heating. An Asylum Research (Santa Barbara, CA) MFP-3D AFM was used.

In all experiments, heater temperatures were tested in an randomly alternating order to distinguish effects of temperature from other effects such as drift or potential tip wear, which would be progressive. Air temperature and humidity were continuously monitored (Humidity Meter 11-661-21, Fisher Scientific, Waltham, MA) and were approximately 21 °C and 25−35% RH, respectively, for all tests performed in air. For the tests in dry nitrogen, the samples were prepared as described above and placed inside a BioHeater closed fluid cell from Asylum Research. The assembly allowed for a closed confinement which was flushed with dry nitrogen for at least 1 h before and during the experiments. While humidity could not be measured during testing, it is expected to be below 3% RH based on past experiments under similar conditions.

To determine the temperature dependence of friction, both constant normal load and variable normal load experiments were conducted. Constant load experiments were performed at an externally applied normal load of 112 nN. The scan area was 100 × 100 nm^2, and the scan rate was 2 Hz for 512 lines. Before staring a scan at this size, a 1 × 1 μm^2 scan was performed to ensure that the test area was homogeneous and did not give rise to unusual friction signals due to roughness or contamination. Tests were carried out for the unheated state (no applied voltage to the cantilever) and at nine different voltages which corresponded to heater temperatures between approximately 110 and 790 °C at separations of approximately 80 °C in a randomly alternating fashion: 705, 110, 620, 195, 535, 280, 450, 365, and 790 °C. Any twisting and bending of the cantilever with voltage was accounted for by centering the AFM's photodiode at each heater temperature with the tip retracted from the surface. The first and last experiments were performed at room temperature to rule out tip wear influencing the data. As a further check for tip wear, the tip was scanned over an ultrananocrystalline diamond (UNCD) surface before and after each set of experiments[50] at a low applied load. From these scans, the tip reconstruction algorithm of the SPIP software for AFM analysis (ImageMetrology, Hørsholm, Denmark) could be used to estimate the tip shape.[51] It was found that, over the course of one set of experiments, there was no detectable change in tip radius.

For the experiments with variable normal force, a script was written for the IgorPro software controlling the MFP-3D AFM. This script changed the normal force feedback set point after every scan line, decreasing the load from positive values until the tip pulled off from the sample. As with the constant load experiments, the scan consisted of 512 lines across a 100 × 100 nm^2 region at a scan rate of 2 Hz.

To investigate the sliding speed dependence of friction, measurements at 10 different speeds ranging from 40 to 7800 nm/s and at a constant load of 112 nN were performed. For these tests, the scan line width was 100 nm, and 128 lines were scanned.

Our previous results for silicon samples indicated that heating the tip in a humid environment causes a capillary meniscus to be formed at the tip−sample contact, and the formation of this meniscus follows Arrhenius kinetics.[15] To further study the effect of the developing capillary on friction at different temperatures, experiments were performed where the heater temperature was increased while scanning for 512 lines at 2 Hz. To investigate the effect of sliding speed on the real-time measurements, additional experiments at 26.04 Hz were performed. All these tests started with zero applied voltage to the cantilever. After several scan lines, the voltage was switched on. The heater reached its temperature with a time constant of less than 1 ms.[16,44] After friction had reached a steady value, the voltage was switched off again. These experiments were performed for three select heater temperatures, in both dry nitrogen and ambient environment. Due to the real-time nature of this method, the twisting and bending of the cantilever could not be corrected for during the measurement. Because of this, only probes which bent upward (away from the sample, thus reducing the applied normal load) upon heating were selected for these experiments. This ensured that any increase in friction can be attributed to genuine thermal effects and not to an increase in normal load. The effect of cantilever twist was eliminated by calculating friction values as half of the difference between the lateral trace and retrace signal (friction loop), such that an overall offset in the lateral signal would not affect the measured friction force. Adhesion between tip and sample was determined by force distance−curve experiments. These were conducted at the same temperatures as the friction measurements, and at least ten individual separation experiments per temperature were performed at a rate of 1 Hz. All measured data were analyzed using custom MatLab (MathWorks, Natick, MA) code.[52]

It is not possible to experimentally determine the temperature at the nanoscale contact between tip and substrate directly. The temperature increase at the contact depends on the tip size and the thermal conductivity ratio of the tip and sample material.[17] Applying a blind reconstruction algorithm for the tip shape resulted in average radius of 22 nm. Using 20 nm for the tip radius and a thermal conductivity ratio of 0.05, the temperature increase at the contact is calculated to be approximately 30% of the temperature rise at the heater, based on a detailed thermal model created for this specific thermal probe method.[17] Thus, we estimate that tip temperatures ranged from room temperature to approximately 255 ± 25 °C. The uncertainty in the temperature rise has many sources, including the exact contact pressure and radius, as well as assumptions made in deriving the theory. It is thus difficult to give a precise number for the expected error in tip temperature, but we conservatively select ±10%.

Conflict of Interest: The authors declare no competing financial interest.

Acknowledgment. This research was partially supported by the Nano/Bio Interface Center through the National Science Foundation NSEC DMR08-32802. Acknowledgment is made to the Donors of the American Chemical Society Petroleum Research Fund for partial support of this research as well as to DARPA's program on Tip-Based Nanofabrication. C.G. acknowledges a Feodor Lynen Fellowship of the Alexander von Humboldt foundation. We thank T. Das and Prof. Y. Goldman

for assistance with the Asylum AFM, and Dr. M. Brukman for help with the variable load experiments. Contact angle measurements were carried out in Prof. S. Yang's group at the University of Pennsylvania. We thank Prof. J.L. Lukes and Prof. E. Charlaix for useful discussions.

Supporting Information Available: Figures S1−S3. This material is available free of charge *via* the Internet at http://pubs.acs.org.

REFERENCES AND NOTES

1. Schirmeisen, A.; Jansen, L.; Holscher, H.; Fuchs, H. Temperature Dependence of Point Contact Friction on Silicon. *Appl. Phys. Lett.* **2006**, *88*, 123108.
2. Brukman, M. J.; Gao, G. T.; Nemanich, R. J.; Harrison, J. A. Temperature Dependence of Single-Asperity Diamond-Diamond Friction Elucidated Using AFM and MD Simulations. *J. Phys. Chem. C* **2008**, *112*, 9358–9369.
3. Krylov, S. Y.; Frenken, J. W. M. The Crucial Role of Temperature in Atomic Scale Friction. *J. Phys.: Condens. Matter* **2008**, *20*, 354003.
4. Zhao, X.; Hamilton, M.; Sawyer, W. G.; Perry, S. S. Thermally Activated Friction. *Tribol. Lett.* **2007**, *27*, 113.
5. Zhao, X. Y.; Phillpot, S. R.; Sawyer, W. G.; Sinnott, S. B.; Perry, S. S. Transition from Thermal to Athermal Friction under Cryogenic Conditions. *Phys. Rev. Lett.* **2009**, *102*, 186102.
6. Tshiprut, Z.; Zelner, S.; Urbakh, M. Temperature-Induced Enhancement of Nanoscale Friction. *Phys. Rev. Lett.* **2009**, *102*, 136102.
7. Binnig, G.; Quate, C. F.; Gerber, C. Atomic Force Microscope. *Phys. Rev. Lett.* **1986**, *56*, 930–933.
8. Mate, C. M.; McClelland, G. M.; Erlandsson, R.; Chiang, S. Atomic-Scale Friction of a Tungsten Tip on a Graphite Surface. *Phys. Rev. Lett.* **1987**, *59*, 1942–1945.
9. Carpick, R. W.; Salmeron, M. Scratching the Surface: Fundamental Investigations of Tribology with Atomic Force Microscopy. *Chem. Rev.* **1997**, *97*, 1163–1194.
10. Szlufarska, I.; Chandross, M.; Carpick, R. W. Recent Advances in Single-Asperity Nanotribology. *J. Phys. D: Appl. Phys.* **2008**, *41*, 123001.
11. Jansen, L.; Schirmeisen, A.; Hedrick, J. L.; Lantz, M. A.; Knoll, A.; Cannara, R.; Gotsmann, B. Nanoscale Frictional Dissipation into Shear-Stressed Polymer Relaxations. *Phys. Rev. Lett.* **2009**, *102*, 236101.
12. Bao, H. F.; Li, X. X. A Heater-Integrated Scanning Probe Microscopy Probe Array with Different Tip Radii for Study of Micro-Nanosize Effects on Silicon-Tip/Polymer-Film Friction. *Rev. Sci. Instrum.* **2008**, *79*, 033701.
13. Szoszkiewicz, R.; Riedo, E. Nucleation Time of Nanoscale Water Bridges. *Phys. Rev. Lett.* **2005**, *95*, 135502.
14. Szoszkiewicz, R.; Riedo, E. Nanoscopic Friction as a Probe of Local Phase Transitions. *Appl. Phys. Lett.* **2005**, *87*, 033105.
15. Greiner, C.; Felts, J. R.; Dai, Z.; King, W. P.; Carpick, R. W. Local Nanoscale Heating Moduates Single-Asperity Friction. *Nano Lett.* **2010**, *10*, 4640–4645.
16. Lee, J.; Beechem, T.; Wright, T. L.; Nelson, B. A.; Graham, S.; King, W. P. Electrical, Thermal and Mechanical Characterization of Sililcon Microcantilever Heaters. *J. Microelectromech. Syst.* **2006**, *15*, 1644–1655.
17. Nelson, B. A.; King, W. P. Modeling and Simulation of the Interface Temperature between a Heated Silicon Tip and a Substrate. *Nanoscale Microscale Thermophys. Eng.* **2008**, *12*, 98–115.
18. Romig, A. D.; Dugger, M. T.; McWhorter, P. J. Materials Issues in Microelectromechanical Devices: Science, Engineering, Manufacturability and Reliability. *Acta Mater.* **2003**, *51*, 5837–5866.
19. Azevedo, R. G.; Jones, D. G.; Jog, A. V.; Jamshidi, B.; Myers, D. R.; Chen, L.; Fu, X. A.; Mehregany, M.; Wijesundara, M. B. J.; Pisano, A. P. A SiC MEMS Resonant Strain Sensor for Harsh Environment Applications. *IEEE Sens. J.* **2007**, *7*, 568–576.
20. Patil, A. C.; Fu, X. A.; Mehregany, M.; Garverick, S. L. 6H-SiC JFETs for 450 °C Differential Sensing Application. *J. Microelectromech. Syst.* **2009**, *18*, 950–961.
21. Lee, T. H.; Bhunia, S.; Mehregany, M. Electromechanical Computing at 500 Degrees C with Silicon Carbide. *Science* **2010**, *329*, 1316–1318.
22. Piner, R. D.; Zhu, J.; Xu, F.; Hong, S. H.; Mirkin, C. A. "Dip-Pen" Nanolithography. *Science* **1999**, *283*, 661–663.
23. Ginger, D. S.; Zhang, H.; Mirkin, C. A. The Evolution of Dip-Pen Nanolithography. *Angew. Chem., Int. Ed.* **2004**, *43*, 30–45.
24. Sirghi, L. Transport Mechanisms in Capillary Condensation of Water at a Single-Asperity Nanoscopic Contact. *Langmuir* **2012**, *28*, 2558–2566.
25. Jang, J.; Schatz, G. C.; Ratner, M. A. Capillary Force on a Nanoscale Tip in Dip-Pen Nanolithography. *Phys. Rev. Lett.* **2003**, *90*, 156104.
26. Jang, J. Y.; Schatz, G. C.; Ratner, M. A. How Narrow Can a Meniscus Be?. *Phys. Rev. Lett.* **2004**, *92*, 085504.
27. Jang, J.; Ratner, M. A.; Schatz, G. C. Atomic-Scale Roughness Effect on Capillary Force in Atomic Force Microscopy. *J. Phys. Chem. B* **2006**, *110*, 659–662.
28. Weeks, B. L.; Vaughn, M. W.; DeYoreo, J. J. Direct Imaging of Meniscus Formation in Atomic Force Microscopy Using Environmental Scanning Electron Microscopy. *Langmuir* **2005**, *21*, 8096–8098.
29. Weeks, B. L.; DeYoreo, J. J. Dynamic Meniscus Growth at a Scanning Probe Tip in Contact with a Gold Substrate. *J. Phys. Chem. B* **2006**, *110*, 10231–10233.
30. Restagno, F.; Bocquet, L.; Biben, T. Metastability and Nucleation in Capillary Condensation. *Phys. Rev. Lett.* **2000**, *84*, 2433–2436.
31. Carpick, R. W.; Batteas, J. D.; de Boer, M. P. In *Handbook of Nanotechnology*; Bhushan, B., Ed.; Springer: New York, 2006.
32. Opitz, A.; Ahmed, S. I. U.; Scherge, M.; Schaefer, J. A. Nanofriction Mechanisms Derived from the Dependence of Friction on Load and Sliding Velocity from Air to UHV on Hydrophilic Silicon. *Tribol. Lett.* **2005**, *20*, 229–234.
33. Gun'ko, V. M.; Zarko, V. I.; Chuikov, B. A.; Dudnik, V. V.; Ptushinskii, Y. G.; Voronin, E. F.; Pakhlov, E. M.; Chuiko, A. A. Temperature-Programmed Desorption of Water from Fumed Silica, Titania, Silica/Titania, and Silica/Alumina. *Int. J. Mass Spectrom.* **1998**, *172*, 161–179.
34. Li, X.; Li, Z.; Xia, Q. B.; Xi, H. X. Effects of Pore Sizes of Porous Silica Gels on Desorption Activation Energy of Water Vapour. *Appl. Therm. Eng.* **2007**, *27*, 869–876.
35. Tomlinson, G. A. A Molecular Theory of Friction. *Philos. Mag. Ser.* **1929**, *7*, 905–939.
36. Prandtl, L. Ein Gedankenmodell zur Kinetischen Theorie der Festen Körper. *Z. Angew. Math. Mech.* **1928**, *8*, 85.
37. Gnecco, E.; Bennewitz, R.; Gyalog, T.; Loppacher, C.; Bammerlin, M.; Meyer, E.; Guntherodt, H. J. Velocity Dependence of Atomic Friction. *Phys. Rev. Lett.* **2000**, *84*, 1172–1175.
38. Bennewitz, R.; Gnecco, E.; Gyalog, T.; Meyer, E. Atomic Friction Studies on Well-Defined Surfaces. *Tribol. Lett.* **2001**, *10*, 51–56.
39. Krylov, S. Y.; Jinesh, K. B.; Valk, H.; Dienwiebel, M.; Frenken, J. W. M. Thermally Induced Suppression of Friction at the Atomic Scale. *Phys. Rev. E* **2005**, *71*, 065101.
40. Li, Q. Y.; Dong, Y. L.; Perez, D.; Martini, A.; Carpick, R. W. Speed Dependence of Atomic Stick-Slip Friction in Optimally Matched Experiments and Molecular Dynamics Simulations. *Phys. Rev. Lett.* **2011**, *106*, 126101.
41. Szoszkiewicz, R.; Riedo, E. Nucleation Time of Nanoscale Water Bridges. *Phys. Rev. Lett.* **2005**, *95*, 135502; **2007**, *98*, 139904 (erratum).
42. Riedo, E.; Levy, F.; Brune, H. Kinetics of Capillary Condensation in Nanoscopic Sliding Friction. *Phys. Rev. Lett.* **2002**, *88*, 185505.
43. Fletcher, P. C.; Felts, J. R.; Dai, Z.; Jacobs, T. D.; Zeng, H.; Lee, W.; Sheehan, P. E.; Carlisle, J. A.; Carpick, R. W.; King, W. P. Wear-Resistant Diamond Nanoprobe Tips with Integrated Silicon Heater for Tip-Based Nanomanufacturing. *ACS Nano* **2010**, *4*, 3338–3344.

44. Lee, J.; King, W. P. Microcantilever Hotplates: Design, Fabrication, and Characterization. *Sens. Actuators, A* **2007**, *136*, 291–298.
45. King, W. P.; Kenny, T. W.; Goodson, K. E.; Cross, G.; Despont, M.; Durig, U.; Rothuizen, H.; Binnig, G. K.; Vettiger, P. Atomic Force Microscope Cantilevers for Combined Thermomechanical Data Writing and Reading. *Appl. Phys. Lett.* **2001**, *78*, 1300–1302.
46. Nelson, B. A.; King, W. P. Temperature Calibration of Heated Silicon Atomic Force Microscope Cantilevers. *Sens. Actuators, A* **2007**, *140*, 51–59.
47. Tortonese, M.; Kirk, M. Characterization of Application Specific Probes for SPMs. *Proc. SPIE* **1997**, *3009*, 53–60.
48. Ohler, B. Practical Advice on the Determination of Cantilever Spring Constants. Veeco Calibration Instructions 2007.
49. Li, Q.; Kim, K. S.; Rydberg, A. Lateral Force Calibration of an Atomic Force Microscope with a Diamagnetic Levitation Spring System. *Rev. Sci. Instrum.* **2006**, *77*, 065105.
50. Sumant, A. V.; Grierson, D. S.; Gerbi, J. E.; Birrell, J.; Lanke, U. D.; Auciello, O.; Carlisle, J. A.; Carpick, R. W. Toward the Ultimate Tribological Interface: Surface Chemistry and Nanotribology of Ultrananocrystalline Diamond. *Adv. Mater.* **2005**, *17*, 1039.
51. Villarrubia, J. S. Algorithms for Scanned Probe Microscope Image Simulation, Surface Reconstruction, and Tip Estimation. *J. Res. Natl. Inst. Stand. Technol.* **1997**, *102*, 425–454.
52. http://nanoprobenetwork.org/welcome-to-the-carpick-labs-software-toolbox.